ChemComm

COMMUNICATION

View Article Online
View Journal | View Issue

Cite this: *Chem. Commun.*, 2024, **60**, 3182

Received 24th November 2023,
Accepted 19th February 2024

DOI: 10.1039/d3cc05766f

rsc.li/chemcomm

Rapid synthesis of Pt(0) motors-microscrolls on a nickel surface *via* H_2PtCl_6-induced galvanic replacement reaction†

Valeri Tolstoy,*[a] Kirill Nikitin,[a] Aleksei Kuzin,[bc] Fenyang Zhu,[c] Xing Li,[c] Gregory Goltsman,[d] Dmitry Gorin,[b] Gaoshan Huang,*[c] Alexander A. Solovev[c] and Yongfeng Mei[c]

In this study, Pt(0) microscrolls are synthesized on polished Ni *via* galvanic replacement reaction (GRR). Employing *in situ* optical microscopy, the dynamic motion of the catalytic microscrolls as micromotors in H_2O_2 solutions is revealed. This method offers a rapid fabrication of scrolls from diverse noble metals and alloys.

The fabrication of catalytic microscrolls or micromotors has witnessed a variety of innovative methods, each contributing to the advancement of microscale propulsion systems. One of the pioneering methods involved the use of rolled-up nanomembranes to create microtubes with an inner Pt layer for catalysis and an Fe layer for magnetic guidance.[1,2] Another notable approach utilized a strain-engineered nanomembrane method to produce rolled-up Ti/Cr/Pd microtubes, which are integrated on silicon substrates for enhanced oxygen generation from hydrogen peroxide decomposition.[3] Pushing the boundaries of fabrication techniques, researchers have employed high-power LED writing and two-photon absorption 3D laser lithography, enabling the production of micromotors with intricate geometrical features and enhanced functionalities.[4] Additionally, a template-assisted approach is introduced to fabricate conical-shaped tubular microengines with a bimetallic (Pt/Au) structure by electroplating onto an etched silver wire template.[5] A one-step and scalable method to construct self-propelled tubular micromotors by using magnetic covalent–organic frameworks (MCOFs) as functional materials was demonstrated for sensing, catalysis, and drug delivery.[6] Another study explored the fabrication of thermo-responsive microgels using a microfluidic chip, involving materials like Poly(ethylene glycol) diacrylate (PEGDA), Poly(N-isopropylacrylamide) (PNIPAm), and dextran, and demonstrates their dynamic shrinking, swelling, and movement responses to temperature changes, suggesting potential applications in targeted drug delivery and micromotor systems.[7] As the field continues to evolve, novel diverse fabrication methods underscore the potential and versatility of catalytic micromotors in various applications.[8]

The galvanic replacement reaction on the surface of Ni in an H_2PtCl_6 solution is known to be relatively well-studied and is utilized in the creation of new electrocatalysts for water electrolysis, among other applications such as catalysts. In studies, this reaction is employed to produce partially "twisted" Pt(0) microscrolls on the Ni surface.[9] It is demonstrated that such microscrolls can be employed as electrocatalysts for the hydrogen evolution reaction (HER) during water electrolysis and as substrates for surface-enhanced Raman spectroscopy (SERS).[10] It is observed that when Ni is brought into contact with the H_2PtCl_6 solution, a GRR reaction occurs. Ni(0) surface atoms are oxidized to Ni(II) and are transitioned into the solution, while the reduction of Pt(IV) cations from the H_2PtCl_6 composition to Pt(0) and their deposition on the Ni surface takes place. In the aforementioned studies, experimental data on the morphology of such microscrolls are provided. However, the influence of various synthesis conditions on the formation of an array of such microscrolls on the Ni surface is not analysed. Furthermore, an adequate model of the processes occurring on the surface is not constructed. The main hypothesis explaining the formation of such microscrolls is posited to be the result of the cracking of Pt(0) layers during the drying of samples in the air. Subsequently, the process of the formation of microscrolls in H_2PtCl_6 solutions of varying concentrations and with different Ni substrate treatment durations can be investigated.

In this study, the characteristics of Pt(0) microscroll formation using the GRR on the surface of chemically polished Ni are investigated for the first time. Observations are made under *in situ* conditions using an optical microscope of a droplet of the reactant solution on the Ni surface. It is demonstrated that

[a] *Saint Petersburg State University, Institute of Chemistry, 26 Universitetskii Prospect, Petergof, St. Petersburg, 198504, Russia. E-mail: v.tolstoy@spbu.ru*
[b] *Center for Photonic Science and Engineering, Skolkovo Institute of Science and Technology, 3 Nobel Str, Moscow, 121205, Russia*
[c] *Department of Materials Science & State Key Laboratory of Molecular Engineering of Polymers, Fudan University, Shanghai, 200433, P. R. China. E-mail: gshuang@fudan.edu.cn*
[d] *Department of Physics, Moscow State Pedagogical University, 119992, Russia*

† Electronic supplementary information (ESI) available. See DOI: https://doi.org/10.1039/d3cc05766f

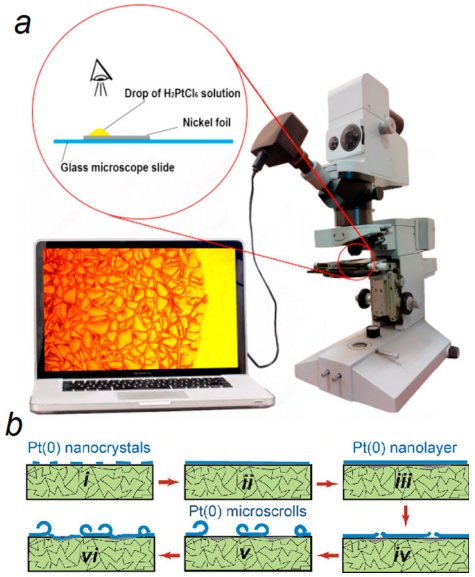

Fig. 1 Optical microscopy and microscroll formation process. (a) Schematic and actual setup for *in situ* optical microscopy to observe tube formation on the Ni surface using a drop of H_2PtCl_6 solution. (b) Different stages of Pt(0) microscroll development (i)–(vi), from Pt(0) nanocrystals and nanolayer formation to the creation of Pt(0) microscrolls on the Ni substrate.

catalytic micromotor properties in an H_2O_2 solution are exhibited by the Pt(0) microscrolls synthesized under these conditions. Next, the approach can be potentially used for the fabrication of microscrolls consisting of various noble metals and their alloys. Potential applications of microscrolls are shown for catalytic micromotors, self-propelling in fuel solutions.

Initial experiments have revealed that the partially formed microscrolls emerging on the Ni surface possess a longitudinal dimension of several micrometers. Therefore, for *in situ* examination of their formation processes, optical microscopy can be employed, and studies are conducted directly within a droplet of the H_2PtCl_6 solution applied to the Ni surface (Fig. 1, Video 1, ESI†). The obtained results indicate that the cracking of the Pt(0) layer on the surface and the subsequent microscroll formation commence at the Ni-solution interface, specifically in the region where the droplet contacts the Ni. When a 0.005 M H_2PtCl_6 solution is used, the initial micro-cracks appear on the surface after approximately 4 min of Ni contact with the solution droplet. As the contact time increases, the area of the Pt(0) layer experiencing cracking expands, and after 10–12 min, it essentially equals the entire droplet contact area with the Ni surface. Extending the treatment time to 14 min results in the formation of an array of partially formed microscrolls on the Ni surface (Fig. 1b).

Based on the entirety of the experimental data, a model for the formation of microscrolls on the Ni surface can be constructed. In the initial stage of treatment in the H_2PtCl_6 solution, a non-continuous layer of Pt(0) forms first, followed by a continuous porous layer of Pt(0) (Fig. 1b). Various stages of Pt(0) microscroll formation take place on the Ni surface: formation of a non-continuous layer of Pt(0) nanocrystals (Fig. 1b(i)), formation of a continuous porous layer of Pt(0) nanocrystals (Fig. 1b(ii)), increase in the thickness of this layer and partial dissolution of Ni beneath the Pt(0) layer (Fig. 1b(iii)), cracking of the Pt(0) layer (Fig. 1b(iv)), partial coiling (Fig. 1b(v)), and formation of a new Pt(0) layer on the Pt surface that is free from the "coiled" layer (Fig. 1b(vi)). This layer is permeable to $PtCl_6^{2-}$ anions and Ni^{2+}_{aq} cations, leading to the formation of unique micron-sized voids on specific parts of the Ni surface, such as at the contact zones of its microcrystals. This results in reduced adhesion of the Pt(0) layer in these areas. The formation of microvoids is believed to be a consequence of the fact that the reduction of one Pt(0) atom requires 4 electrons, while the oxidation of one Ni(0) atom yields only 2 electrons. In other words, for every Pt(0) atom deposited on the surface, two Ni_{aq}^{2+} cations are released into the solution. The presence of voids and internal stresses in the Pt(0) layer, due to the porosity gradient, leads to the cracking and partial coiling of this layer at a certain stage of the reaction, specifically after 4 min of contact between Ni and a 0.005 M H_2PtCl_6 solution (Fig. S1, ESI†). The formed microscrolls remain on the Ni surface since microvoids do not form across its entire surface. If the galvanic replacement reaction (GRR) is conducted in a more concentrated solution, the areas of the substrate that become free from the planar Pt(0) layer after coiling re-enter the GRR, leading to the formation of a new planar layer, which over time cracks and rolls-up. Our experience indicates that when treated with a 0.2 M solution, areas on the surface can be identified that undergo the aforementioned sequential reactions, cracking, and rolling up to 3–4 times.

A more systematic morphological characterization of microscrolls is derived from the analysis of scanning electron microscopy (SEM) micrographs taken from a series of Ni samples treated in the H_2PtCl_6 solution (Fig. 2). For instance, the formation of the initial Pt(0) nanocrystals is noticeable on the polycrystalline Ni surface after 10 s of treatment in the solution (Fig. 2a). Further treatment for 20 s significantly increases the number and size of the crystals (Fig. 2b). After 40 s of treatment, a continuous Pt(0) layer forms, containing individual pores (Fig. 2c) through which, presumably, both the reagent's partial entry into the reaction zone and the removal of reaction products occur. Subjecting the Ni to the reagent solution for 4 min leads to the cracking of the Pt(0) layer and the emergence of the first partially curled microscrolls (Fig. 2d). Prolonged contact of the Ni surface for 20 min increases the number of microscrolls and the degree of their "twisting" (Fig. 2e). Subsequently, the morphology of the array of microscrolls essentially remains unchanged (Fig. 2f). High-resolution transmission electron microscopy (HRTEM) analysis has revealed that the walls of such microscrolls are composed of agglomerates of Pt(0) nanocrystals with a size of approximately 5 nm (Fig. 2g). The composition of the tubular walls was also identified using energy dispersive X-ray spectroscopy (EDX) (Fig. 2h), further confirming the composition of the microscroll walls as Pt(0). The thickness of the microscroll walls, formed during 10 min, is around 100 nm (Fig. S2c, ESI†). As determined from a series of additional experiments, the thickness of the microscroll walls depends on the contact time of Ni with the reagent solution, ranging from 50 nm for a sample treated for 4 min to 180 nm for a sample resulting from a 20-min reagent contact (not shown). Upon analyzing the SEM images, it is noteworthy that the external surface morphology of the

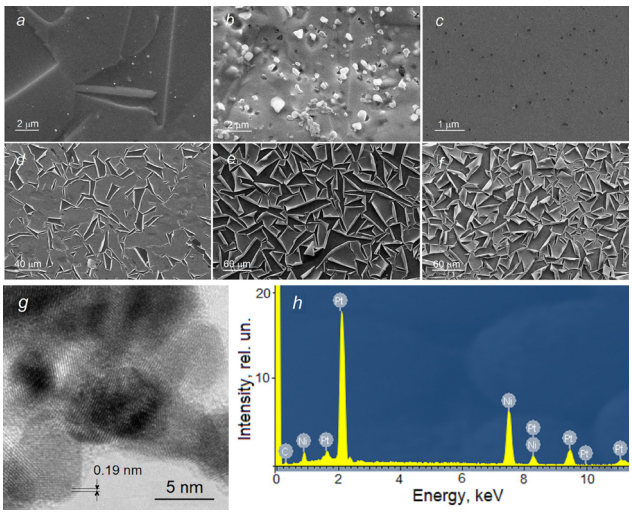

Fig. 2 SEM images of Pt(0) microscrolls. (a)–(f) SEM micrographs showing the evolution of the Ni surface morphology with increased treatment times in H_2PtCl_6 solution (10, 20, and 40 s; 4, 20, and 60 min respectively; $C_{H_2PtCl_6}$ = 0.005 M). (g) HRTEM micrograph of a Pt(0) microscroll wall formed after 10 minutes in H_2PtCl_6 solution. (h) Corresponding EDX spectrum confirming the elemental composition of the microscroll wall.

microscroll differs from its internal counterpart (Fig. S2c and d, ESI†). Specifically, the internal surface features numerous predominantly vertically oriented conical prisms, which significantly increase the surface area of the microscroll's inner part. Another crucial observation from the micrograph in Fig. S2c (ESI†) shows the presence of numerous pores within the microscroll wall, which appear at the contact zones of the Pt(0) nanocrystals. Presumably, pores facilitate the diffusion of the reagent to the Ni surface and the removal of reaction products. It is also worth noting that the side of the wall closest to the Ni exhibits a smoother surface and a denser "packing" of Pt(0) nanocrystals compared to the outer side. One plausible explanation for the smoother surface is the relatively high degree of chemical polishing of the Ni, which was carried out in an acid mixture solution during the preliminary sample preparation stage before the deposition of the Pt(0) layer.

With an increase in the concentration of the H_2PtCl_6 solution to 0.2 M, the time until the first appearance of microscrolls decreases to 2 min (Fig. S3a, ESI†), and the entire array of microscrolls is formed during 10 min (Fig. S3a–f, ESI†). Upon close examination of the micrographs, the formation of secondary microscrolls on the Ni surface in the area is observed, where the reaction to form the Pt(0) layer and its subsequent coiling has already occurred. It is most evident in the central region of the micrographs. For instance, in Fig. S3b (ESI†), the coiling of the layer in the center of the image is noticed. Fig. S3c (ESI†) indicates the formation of a new Pt(0) layer on the freed area of the Ni surface, in Fig. S3d (ESI†) – the rolling of this layer, and in Fig. S3e and f (ESI†) – the formation and rolling of a new third layer in this zone. Meanwhile, the microscrolls that have already formed on the surface essentially retain their morphology. Depositing various "patterns" onto the Ni surface can significantly alter the morphology of the Pt(0) layer assembly as a result of the GRR. Specifically, using a laser beam to create special stripes leads to the cracking of the layer along stripes (Fig. S4a and b, ESI†). On the contrary, the use of photolithography leads to the formation on the Ni surface, free from photoresist, of localized areas of Pt(0) (Fig. S4c, ESI†) and their transformation into Pt(0) microscrolls after treatment in HCl solution (Fig. S4d, ESI†).

To obtain a suspension of microscrolls in water, Ni substrates with microscroll layers are treated in concentrated HCl for 10 min Subsequently, different fractions of microscrolls are separated through sedimentation. SEM micrographs depict one of the fractions of such a sediment (Fig. S5, ESI†). Compared with the micrographs (Fig. 2e and f) that characterize the microscrolls on the Ni surface, it can be inferred that the removal of such microscrolls from the Ni surface leads to their further "tightening" and the formation of more refined tubular structures. This effect becomes clear considering that on the Ni surface, the zones of their contact with the surface hinder more significant "rolling" of the microscrolls. It should also be noted that, according to the micrographs presented in Fig. S5 (ESI†), a significant proportion of the obtained microscrolls have a conical shape (Fig. S5c, ESI†).

As a result, the entire set of experimental data obtained serves as a justification for a new, experimentally simple strategy for producing microscrolls with walls made of Pt(0). A distinctive feature of this strategy is the chemical polishing of Ni (Fig. S6a, ESI†), and the application of specific patterns to its surface, which partially dictate the sizes of the microscrolls (Fig. S6b, ESI†). This is followed by treating the Ni surface with an H_2PtCl_6 solution (Fig. S6c, ESI†), allowing it to stand in this solution for the time required to form the microscrolls. Subsequently, a suspension of microscrolls is obtained by treating the samples in an acid solution (Fig. S6d, ESI†). The microscrolls are then partially separated by size during their sedimentation in the solvent during the acid removal stage by water rinsing (Fig. S6e, ESI†). Preliminary experiments also indicate that microscrolls of other noble metals and their alloys can be obtained on the surface of chemically polished Ni under GRR conditions. However, these experiments are beyond the scope of our current article.

The ability of microscrolls to self-propel, obtained after treating the Ni surface with a pattern previously applied by photolithography, can be assessed by considering the results shown in ESI† Video 2 and 3. Fig. 3 shows an analysis of the kinematic behaviour of catalytic microscrolls in an aqueous hydrogen peroxide (H_2O_2) solution with added SDS surfactant. Fig. 3a shows micrographs capturing the progressive motion of the micromotor. The micromotor changes its position, showing a transformation from linear, to circular and to helical trajectories.

Fig. 3b illustrates the spatial trajectory of the micromotor, with blue circles representing the position of an individual micromotor. The plot reveals a series of looped trajectories, which is characteristic of rotational or spiral motion. Fig. 3c indicates the instantaneous velocity of the micromotor as a function of time. Despite minor fluctuations, the velocity appears to fluctuate within a constrained range, implying a stable propulsion velocity driven by ejecting oxygen microbubbles due to the decomposition of H_2O_2. Fig. 3d demonstrates the displacement (approximately 6 mm) of the scroll-micromotor over the elapsed time of 13 s.

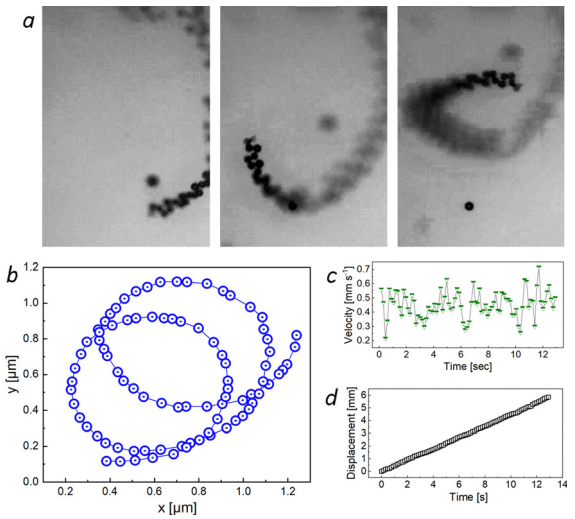

Fig. 3 Motion analysis of an individual tubular catalytic micromotor in H_2O_2 solution. (a) Temporal micrograph sequence showing the motion of the micromotor. (b) Tracked motion illustrating the micromotor's looping trajectory, and (c) velocity fluctuations over time. (d) A displacement recorded during 13 s, confirming consistent motion.

These values indicate a speed of microscroll movement of approximately 460 μm s^{-1}. This magnitude is about 10–20 percent higher than the velocities of Pt(0) microtubes achieved in previous studies[6,11] in H_2O_2 solutions with a similar concentration, and it is noteworthy that the authors of these studies used surfactant solutions with a concentration 50–100 times higher to achieve greater mobility of the microtubes. A similar speed of 420 μm s^{-1} was observed for micromotors with three-layer walls made of Au–Ni–Pt nanolayers,[12] but they were obtained using a multistage template synthesis. The linear nature of the displacement–time graph suggests a constant mean speed over the observed duration, confirming uniform motion in terms of average translational displacement. Subsequently, it is revealed that the catalytic microscrolls execute a controlled motion characterized by motion path, velocity and displacement.

In summary, this research elucidates a new approach for the synthesis of Pt(0) microscrolls, spotlighting the *in situ* microscopy technique to investigate their formation dynamics on Ni substrates. Experiments unveil that the interaction of chemically refined Ni with aqueous H_2PtCl_6 solutions initiates a GRR, leading to the formation of a Pt(0) layer. This layer exhibits a distinct density gradient orthogonal to the substrate, a phenomenon underpinned by the migration of Ni(II) cations into the solution. This process, occurring at a ratio of two Ni(II) cations for every Pt(0) atom precipitated, gives rise to voids beneath the Pt(0) layer, subsequently triggering its fracturing and morphological evolution into microscrolls. This transformation is hallmarked by the rolling of the external facet of the Pt(0) layer inwards. Furthermore, our study identifies that an excess of H_2PtCl_6 in the solution can induce a secondary GRR phase on freshly exposed substrate areas, leading to the formation of new microscrolls interspersed among the initial ones. Moreover, strategic patterning on the Ni substrate, *via* techniques like photolithography or laser processing, can potentially manipulate the geometrical dimensions of the resulting microscrolls. Following structure formation, Pt(0) microscrolls can be delicately separated from the substrate through HCl treatment, yielding isolated microscrolls in colloidal suspensions, which exhibit pronounced micromotor behaviours in H_2O_2 solutions. A high surface area of the microscrolls' interior facilitates efficient oxygen release and formation of microbubbles. This study opens new directions for synthesizing microscrolls from various noble metals and alloys, specifically under tailored GRR conditions on chemically refined Ni substrates.

This work was supported by the National Key Technologies R&D Program of China (2021YFA0715302), the National Natural Science Foundation of China (52150610489), and the Science and Technology Commission of Shanghai Municipality (22ZR1405000). In addition, the authors are grateful to the Centers for Laser Research and Nanotechnology, St. Petersburg State University, Russian Federation, for assistance in the study of the samples, as well as Dr M. Kaneva and Prof. A. Povolotsky for participation in the experiments. The model of chemical processes on the Ni surface was built within the framework of the Russian Science Foundation project #23-19-00566. Large language model GPT was instrumental in refining the early versions of the manuscript.

Conflicts of interest

There are no conflicts to declare.

References

1 Y. Mei, G. Huang, A. A. Solovev, E. B. Ureña, I. Mönch, F. Ding, T. Reindl, R. K. Fu, P. K. Chu and O. G. Schmidt, *Adv. Mater.*, 2008, **20**, 4085–4090.
2 A. A. Solovev, Y. Mei, E. Bermúdez Ureña, G. Huang and O. G. Schmidt, *Small*, 2009, **5**, 1688–1692.
3 S. Naeem, F. Naeem, J. Zhang, J. Mujtaba, K. Xu, G. Huang, A. A. Solovev and Y. Mei, *Micromachines*, 2020, **11**, 643.
4 M. Medina-Sánchez, M. Guix, S. Harazim, L. Schwarz and O. G. Schmidt, in 2016 Intern. Conference on Manipulation, Automation and Robotics at Small Scales (MARSS), IEEE, 2016, pp. 1–6.
5 K. M. Manesh, M. Cardona, R. Yuan, M. Clark, D. Kagan, S. Balasubramanian and J. Wang, *ACS Nano*, 2010, **4**, 1799–1804.
6 K. Wang, E. Ma, Z. Hu and H. Wang, *Chem. Commun.*, 2021, **57**, 10528–10531.
7 S. P. Teora, K. H. van der Knaap, S. Keller, S. J. Rijpkema and D. A. Wilson, *Chem. Commun.*, 2022, **58**, 10333–10336.
8 T. Xu, W. Gao, Li-P. Xu, X. Zhang and S. Wang, *Adv. Mater.*, 2017, **29**, 1603250.
9 M. V. Kaneva and V. P. Tolstoy, *Nanosyst.: Phys. Chem., Math.*, 2021, **12**, 630–633.
10 M. V. Kaneva, E. V. Borisov and V. P. Tolstoy, *Nanosyst.: Phys. Chem., Math.*, 2022, **13**, 509–513.
11 H. Wang, J. G. Sheng Moo and M. Pumera, *Nanoscale*, 2014, **6**, 11359–11363.
12 M. Guix, J. Orozco, M. García, W. Gao, S. Sattayasamitsathit, A. Merkoc-i, A. Escarpa and J. Wang, *ACS Nano*, 2012, **6**, 4445–4451.